

Focussing monochromator–Fermi-chopper time-of-flight spectrometer

H. Mutka

Institut Laue–Langevin, 156X, 38042 Grenoble Cedex, France

The operation of a focussing monochromator in a time-of-flight application is examined. The interest of variable focal conditions in association with time-focussing is demonstrated with a simple example. The real instrument is studied with the aid of a simulation routine.

1. Introduction

The gain of intensity in neutron spectrometry with curved crystal monochromators has been recognised a long time ago and focussing perpendicular to the scattering plane of the monochromator is widely applied. In the scattering plane focussing is more awkward because of the wavelength dispersion that depends on the focussing conditions [1]. Constant wavelength focussing is attainable with the restrictive condition of equal distances from source to monochromator and from monochromator to sample. In time-of-flight applications the drawback of dispersive in-plane focussing can be compensated with time-focussing, which permits to recover resolution. This has been done successfully for example in the design of the cold neutron TOF spectrometer IN6 at the ILL [2]. The purpose of the present paper is to examine an application for thermal neutrons.

2. Time-focussing conditions

The simple scheme of fig. 1 shows the main components of a crystal monochromator TOF spectrometer. The Fermi-chopper that sweeps over the monochromator surface transmits a neutron pulse that has a characteristic form in the wavelength–time space. Time-focussing occurs when the constant wavelength time-width Δt_λ is less than the full-time-width $\Delta t_i = \alpha / (2\pi f)$ of the pulse and when the slower ($\lambda > \lambda_{ave}$) neutrons have started earlier: at a later time (or distance) the pulse will have the constant wavelength time-width. The focal condition can be derived by setting equal to Δt_i the difference in flight-times of the slowest and the fastest neutrons that are separated by $\Delta \lambda_i$ in wavelength:

$$\Delta t_i = C(\Delta \lambda_i L_{cs} + \Delta \lambda_f L_{foc})$$

$$= C \Delta \lambda_i (L_{cs} + (\lambda_f/\lambda_i)^3 L_{foc}). \quad (1)$$

Here the constant $C = 252.77 \mu\text{s}/\text{\AA}/\text{m}$. In certain cases it is possible to find approximate analytic expres-

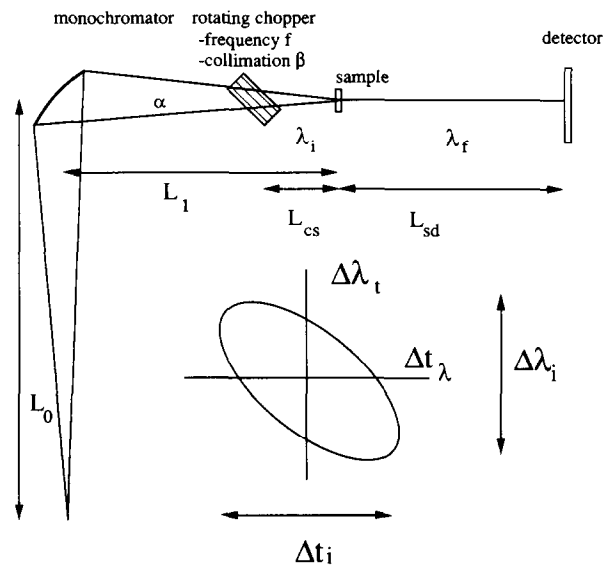


Fig. 1. A schematic presentation of the focussing monochromator–Fermi-chopper spectrometer defining the important parameters and showing the wavelength–time structure of the transmitted neutron pulse.

sions for Δt_i and $\Delta \lambda_i$ in order to obtain a convenient formula for the focal distance L_{foc} ($= L_{sd}$ usually) as a function of the instrument parameters. For example, with a point source at a distance L_0 from a curved monochromator of width w_m that focusses on a point sample at a distance L_1 (the radius of curvature is given by $2/(R \sin \Theta_B) = 1/L_0 + 1/L_1$) one finds

$$\Delta \lambda_i = \lambda_i \cot \Theta_B \Delta \Theta_B$$

$$= 2d_m \cos \Theta_B (w_m/2) \sin \Theta_B (1/L_1 - 1/L_0), \quad (2a)$$

$$\Delta t_i = \alpha / (2\pi f) = w_m \sin \Theta_B / (2\pi f) / L_1, \quad (2b)$$

which gives a focal condition

$$2\pi f_{foc} d_m \cos \Theta_B C (L_{cs} + (\lambda_f/\lambda_i)^3 L_{foc})$$

$$= (1 - L_1/L_0)^{-1}. \quad (3)$$

It is easy to see that monochromatic focussing ($L_0 = L_1$) produces no time-focussing and that varying imaging conditions (L_0, L_1) can control the focus ($f_{\text{foc}}, \lambda_{f,\text{foc}}$). This is an advantage with respect to the limit $L_0 = \infty$, where we recover the IN6 type focal condition that ideally concentrates a parallel beam on a point sample (in practice three overlapping wavelengths from three physically separate monochromators). A very important feature in eq. (3) is the fact that a reduced object distance $L_0 \geq L_1$ permits a higher chopper frequency without a corresponding decrease of the focal distance. This improves the final resolution (Δt_λ) and helps operation at low take-off angles (when $\cos \theta_B \leq 1$). The practical control of the focus will be affected by the properties of the real spectrometer, for example by source size, physical configuration of the curved monochromator and its mosaic distribution, the design of the chopper, sample and detector dimensions, etc. The same factors define also the Δt_λ that will be the ultimate resolution at the focus. Therefore the analytical calculations in limiting cases can be used as guidelines, but should be applied with caution to spectrometer optimization. To overcome this difficulty we have to rely on simulation.

3. Simulation of the spectrometer

Our aim in the simulation was to obtain reliable estimates for the resolution and for the definition of the beam optics. The simulation routine is based on the ray-tracing technique with random choice of initial neutrons. The first trajectory guess defines the beam coming out from the beam-tube. The background chopper system is treated simply from the point of view of geometric transmission. The monochromator assembly consists of a (variable) number of vertical and horizontal pieces of a chosen size and no thickness. The analytical model of Gaussian mosaic distribution is used for the monochromator. The Fermi-chopper has an ideal triangular transmission in time. The sample can be positioned at a variable angle with respect to the incident beam. The detector assembly consists of three rows of ^3He tubes tangent to the scattering cone at a given angle. All elements defining the beam optics, except the circular beam tube, have rectangular cross-sections.

The simulation gives a reliable intensity-resolution evaluation for fixed take-off angle in variable focussing conditions. The neglect of wavelength dependent transmission factors, such as monochromator reflectivity and transmission of the choppers, hinders an accurate estimation of the absolute intensity.

The output of the simulation includes the individual resolution components $\Delta\lambda/\lambda$, $\Delta L/L$ and $\Delta t/t$ that are useful for optimising instrument parameters like the dimensions of elements and distances between them; the number of individual pieces of the mono-

chromator; the mosaic width; etc. It is possible to calculate the energy transfer dependent resolution width at different focussing conditions. For the moment the Q -resolution and its dependence on the focussing has not been included in the calculation.

4. Examples of time-focussing operation

An example of the effect of beam optics on the focussing conditions is depicted in fig. 2 which shows how the transmitted neutron pulse changes form at the chopper when the monochromator curvature is adjusted. The observed (Monte Carlo) time gradient of the wavelength $\Delta\lambda_i/\Delta t_i$ is plotted against the normalised distance from the source focal point to the monochromator. The source has a diameter of 10 cm and it is at a distance of 9.5 m from the monochromator. For

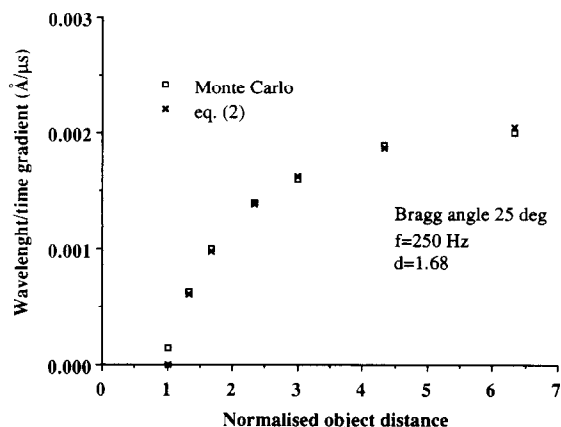


Fig. 2. The wavelength-time gradient of the transmitted pulse versus the normalised object distance L_0/L_1 . Results from the Monte Carlo simulation with realistic parameters compare well with the ideal model of eq. (2).

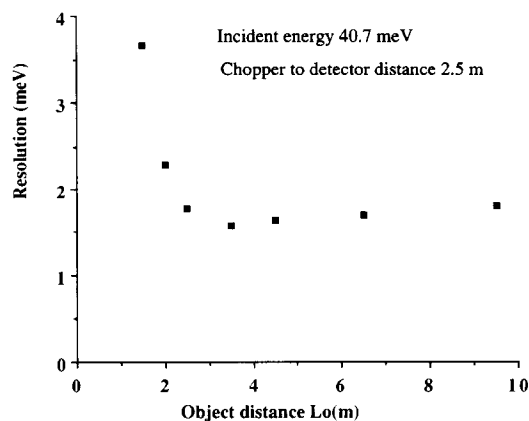


Fig. 3. The elastic resolution at $E_i = 40.7$ meV versus the object distance. Optimal focussing occurs at $L_0 = 2.3 L_1 = 3.5$ m where the $\Delta\lambda/\Delta t$ gradient is 65% of the $L_0 = \infty$ limit, see fig. 2.

comparison we plot the dependence described by the eq. (2), which is valid for a point source.

The dependence of the resolution on the object distance is shown in fig. 3 for an incident energy of 40.7 meV and chopper to detector distance $L_{cs} + L_{sd} = 2.5$ m. The result demonstrates the importance of adjustable horizontal curvature in optimising the resolution.

5. Conclusion

With a simple example and a simulation we have examined the horizontally focussing monochromator in association with time-focussing. With a relatively wide source it is possible to adjust the object plane distance in order to optimise the focal condition for thermal neutron application. The motivation of this study was the evaluation of the resolution and intensity of the new IN4C thermal TOF spectrometer, which is under construction at the ILL. This instrument will have a variable curvature monochromator that gives a

considerable gain of flux on the sample. We can foresee that the present simulation routine will also be useful in the future for the evaluation of optimal operation conditions.

Acknowledgements

It is a pleasure to thank Amir Murani who showed me the way on "the flight path". The assistance of Mr. M. Baudach in programming the curved monochromator simulation was of great help.

References

- [1] A.K. Freund, in: *Imaging Processes and Coherence in Physics*, eds. M. Schlenker, M. Fink, J.P. Goedgeburger, C. Malgrange, J.Ch. Viénot and R.H. Wade, *Lecture Notes in Physics* 112 (Springer, Berlin, 1980) p. 381, and references therein.
- [2] R. Scherm, C. Carlile, J. Dianoux, J. Suck and J. White, *Scientific Report no. 76S235S*, Institut Laue-Langevin, 1976.